Convergence of FDTD and Wavelet-Collocation Modeling of Curved Dielectric Interface With the Effective Dielectric Constant Technique

Masafumi Fujii, Dzianis Lukashevich, Iwata Sakagami, and Peter Russer

***Abstract*—The convergence of the effective dielectric constant (EDC) model of curved dielectric surfaces has been investigated precisely for the finite-difference time-domain (FDTD) as well as for the interpolet-collocation time-domain (ICTD) methods.**

The EDC is computed by solving the Laplace equation of static electric potential by a finite-difference (FD) method for each cell located on the interface of arbitrary dielectric media. The FD solution of the Laplace equation provides an accurate EDC for arbitrary curved interface with even high contrast of the dielectric constants. It has been demonstrated in this paper that the precisely chosen EDC allows both the FDTD and the wavelet-collocation methods to exhibit second-order convergence for the analysis of not only planar but also curved dielectric interfaces.

***Index Terms*—Effective dielectric constant (EDC), finite-difference time-domain (FDTD), wavelet-collocation method.**

I. INTRODUCTION

THE space-discrete electromagnetic field analysis is robust, but is often limited by available computer resources in particular for electrically-large structures which are significantly larger than the wavelength of the major frequency content of the transmitted signal. We have proposed for such problems the interpolet-collocation time-domain (ICTD) method [1]–[3], which uses a large-stencil scheme, and has highly linear numerical dispersion. This method allows relatively coarser discretization compared to e.g., the standard finite-difference time-domain (FDTD) method, thus reducing the number of cells while maintaining the accuracy of the solution.

The disadvantage of such a high-order scheme is the treatment of curved dielectric interfaces; i.e., for coarser discretization, the staircase approximation leads to a large error. It has been demonstrated for a plane dielectric interface that second- order convergence is maintained for the FDTD method if the effective dielectric constants (EDCs) at the interface is determined by arithmetic averaging for tangential electric field nodes, and by harmonic averaging for perpendicular electric field nodes [4], [5]. The interface can thus be located at an arbitrary distance from the grid axes. This concept has been extended to curved dielectric surfaces, and some efficient techniques using the EDC have been proposed [6]–[8]. In [6], the EDC is computed by harmonic averaging in the longitudinal direction of the associated electric field, and arithmetic averaging in the transversal direction. The technique given in [7] uses the similar concept of weighted-volume effective dielectric constant. The simple treatment of the EDC adopted in [8] takes into account simply the location of the intersection between the grid axis and the dielectric interface.

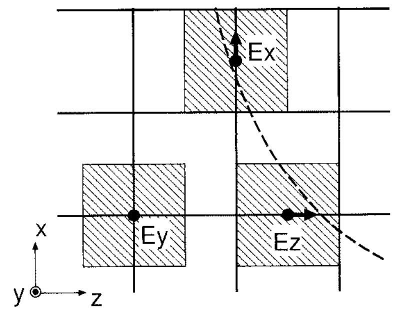

Fig. 1. The 3-D Yee grid and the electric field nodes.

The previous EDC techniques have been reported to provide more accurate results than the staircase approximation. However, the convergence of the techniques has not been clearly demonstrated yet, which is of particular importance to ensure the accuracy when the discretization is refined. Moreover, it is demonstrated that the previous techniques yield some faulty EDCs for a particular example shown in the next section.

Therefore, for the purpose to implement in the ICTD method with relatively coarser discretization than in the standard FDTD, we have adopted the EDC computed by solving the Laplace equation of static electric potential using a finite-difference (FD) method. The computational overhead is not significant because the EDCs are computed only once as a preprocess, which takes only a fraction of time compared to the entire CPU time; the memory requirement for the static FD process is much less than the main FDTD/ICTD computation.

II. COMPARISON OF EFFECTIVE DIELECTRIC CONSTANT TECHNIQUES

We consider structures with curved dielectric interfaces that are parallel to the z-axis of the Cartesian coordinate system. In the three-dimensional (3-D) Yee grid, we focus on the E_x field node and the associated dielectric constant as shown in Fig. 1; the thick lines are the main grid liens, and the hatched region is the unit cell in which the electric field is represented by a node located at its center.

Manuscript received March 10, 2003; revised July 9, 2003. The review of this letter was arranged by Associate Editor Dr. Arvind Sharma.

M. Fujii and I. Sakagami are with the Department of Electric and Electronic Engineering, Toyama University, Toyama-shi, 930-8555 Japan (e-mail: mfujii@eng.toyama-u.ac.jp).

D. Lukashevich and P. Russer are with the Laboratory for High-Frequency Engineering, University of Technology Munich, D-80333 Munich, Germany.

Digital Object Identifier 10.1109/LMWC.2003.819374

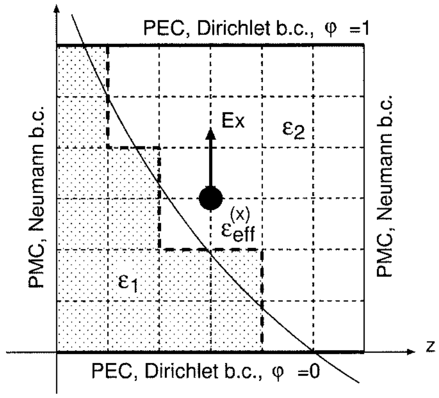

Fig. 2. Parallel plate capacitor with inhomogeneous media.

In order to compute the EDC of such a region, we consider a parallel plate capacitor with two electrodes perpendicular to its representative field. Then the EDC is computed as the ratio of the capacitance of the region to that of the region filled with air. The only approximate factor in this case is the boundary condition for the walls tangential to the field; in this paper we have imposed the Neumann boundary condition. The EDC for E_z is obtained similarly, and that for E_y is obtained by the simple arithmetic averaging of the dielectric constants in the region since the interface has been assumed to be parallel to the E_y field.

Then the necessary task is to compute the capacitance of the parallel plate capacitor with inhomogeneous media as shown in Fig. 2. The governing equation is the Laplace equation for the static electric field

$$\nabla \cdot (\varepsilon \nabla \varphi) = 0 \quad (1)$$

which is solved with the FD method with the over-relaxation Gauss-Seidel iteration procedure. The standard second-order central difference scheme is used for the potential φ, and simple averaging between the neighboring cells is used for the inhomogeneous distribution of ε. In the two-dimensions, for simplicity, the resulting difference equation of an iterative form is given by

$$\varphi_{00}^{n+1} = (1-R)\varphi_{00}^{n} + R\frac{\frac{1}{\Delta x^2}\left(\varepsilon_{h0}\varphi_{10}^{n} + \varepsilon_{\bar{h}0}\varphi_{\bar{1}0}^{n}\right) + \frac{1}{\Delta z^2}\left(\varepsilon_{0h}\varphi_{01}^{n} + \varepsilon_{0\bar{h}}\varphi_{0\bar{1}}^{n}\right)}{2\left(\frac{1}{\Delta x^2} + \frac{1}{\Delta z^2}\right)\varepsilon_{00}} \quad (2)$$

where the over relaxation factor $R = 1.4$ is typically used, and the dielectric constants at the cell boundaries are calculated by

$$\varepsilon_{h0} = \frac{\varepsilon_{hh} + \varepsilon_{h\bar{h}}}{2} \quad (3)$$

$$\varepsilon_{00} = \frac{\varepsilon_{hh} + \varepsilon_{h\bar{h}} + \varepsilon_{\bar{h}h} + \varepsilon_{\bar{h}\bar{h}}}{4} \quad (4)$$

etc., of which subscripts are defined in Fig. 3.

For the simple problem shown in the inset of Fig. 4, we have computed the EDC for the E_x field node with the previously reported techniques [6], [8] and the FD solution of the Laplace equation. The resulting EDCs are shown in Fig. 4 for the case of the dielectric constants $\varepsilon_1 = 38$ and $\varepsilon_2 = 1$.

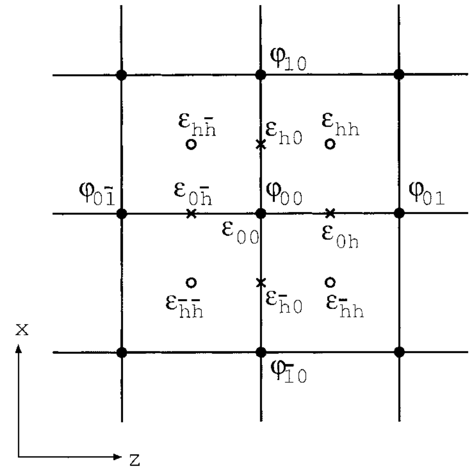

Fig. 3. Definition of the notation of the difference equation. The index "h" denotes 1/2, and the upper bar for the subscripts represents a negative index.

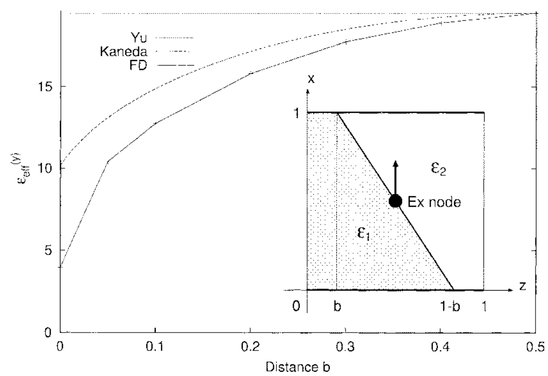

Fig. 4. Example of inhomogeneous cell geometry and the EDCs obtained with the previously reported techniques and the FD method.

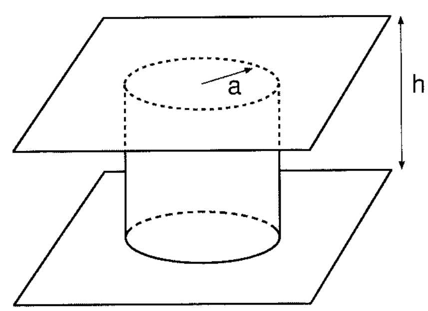

Fig. 5. Analyzed cylindrical dielectric resonator.

Since Yu's approach [8] determines the EDC by the location of the intersection between the grid axis and the curved interface, it leads to a constant EDC for different b in this case. The other technique by Kaneda [6] agrees well with the FD method when the contrast of ε is small, nevertheless it agrees worse in particular for larger contrast with oblique interfaces.

III. Numerical Experiments

In order to investigate the accuracy and the convergence, the EDC technique was applied to a cylindrical dielectric rod resonator sandwiched with parallel metal plates [6] as shown in Fig. 5; the radius and the hight of the cylindrical rod is $a =$

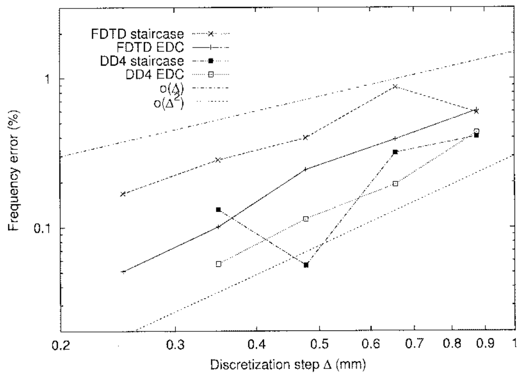

Fig. 6. Resonant frequency error (%) of the HEM_{111} mode of the cylindrical rod resonator. The first and the second-order convergence plots ($o(\Delta)$ and $o(\Delta^2)$, respectively) are also given for reference.

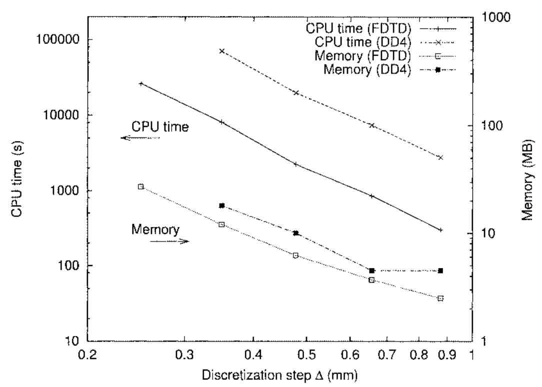

Fig. 7. Required CPU time and the memory.

5.25 mm and $h = 4.6$ mm, respectively; note that the dimensions are dropped in [6], and a wrong height is given in [7]; the dielectric constant of the rod is $\epsilon_r = 38.0$; and the outside of the rod is air. The EDCs were computed with the FD analysis of the Laplace equation; the Yee cells located on the dielectric interface was sub-divided into 20 $\times$ 20 cells, which has been confirmed to be sufficiently accurate by preliminary experiments. Five layers of the perfectly matched layer (PML) were used to surround the $4a \times 4a \times h$ rectangular box region; the dielectric rod is placed at the center; the top and the bottom walls are the perfect electric conductors (PECs). The resonator was analyzed with the standard FDTD and the ICTD method based on the fourth-order Deslauriers-Dubuc interpolation function (DD4) [1]. We analyzed the HEM_{111} resonant mode. The exact resonant frequency is 6.213 958 974 7 GHz, which has been obtained from the analytical dispersion relation.

The discretization steps $\Delta x, \Delta y$, and Δz for the FDTD and the ICTD methods were chosen to be $(a/\Delta, h/\Delta y) = (21, 20)$, $(15, 15), (11, 10), (8, 8)$, and $(6, 6)$, where $\Delta = \Delta x = \Delta z$. The time step was 0.95 of the Courant limit for the FDTD and 0.2 of that of the corresponding FDTD grid for the IC-DD4 scheme. The computation was performed for the maximum time $T_{\max} = 1.0 \times 10^8$ s, which corresponds to 50-period length, sufficient to obtain a convergent resonant frequency by the Fourier transform.

The result of the resonant frequency error is plotted in Fig. 6 as well as the required computer resource in Fig. 7. For the staircase approximation, the FDTD exhibit nearly first-order convergence; with the EDC, the convergence has been improved to second-order. For the IC-DD4 scheme, the convergence has not been obtained for the staircase approximation, whereas second-order convergence is observed with the EDCs; moreover, the accuracy is still higher in the IC-DD4 scheme than in the FDTD with the same discretization. It is emphasized here that, with the EDCs, the FDTD and the ICTD methods provide the second-order accuracy even for curved dielectric interfaces.

The computation has been performed on a personal computer with 300 MHz clock rate and 96 MBytes of memory. The CPU time required for the FD solution of the Laplace equation was approximately 0.1 s per cell, and the total additional time for the EDC process was a few minutes. The ICTD method with DD4 basis function needs more CPU time than the FDTD for the same discretization because the time step is usually chosen to be five times less. Instead of this cost, it provides higher accuracy, reducing the number of cells by a factor of 2 to 4 per dimension. Therefore, the ICTD method is more suitable for electrically-large structures compared to the standard FDTD.

IV. Conclusion

The EDC technique based on the FD solution of the Laplace equation has been applied to the FDTD and the ICTD electromagnetic field analysis. It has been numerically shown that the FDTD and the ICTD methods exhibit second-order convergence even for the curved dielectric interface if the EDC are used; moreover, the ICTD method maintains higher accuracy than the standard FDTD with the same discretization. The IC method will thus be efficient for the analysis of large scale electromagnetic field problems.

References

[1] M. Fujii and W. J. R. Hoefer, "Application of biorthogonal interpolating wavelets to the Galerkin scheme of time dependent Maxwell's equations," *IEEE Microwave Wireless Comp. Lett.*, vol. 11, pp. 22–24, 2001.

[2] ——, "A wavelet formulation of finite difference method: Full vector analysis of optical waveguide junctions," *IEEE J. Quantum Electron.*, vol. 37, pp. 1015–1029, Aug. 2001.

[3] ——, "Interpolating wavelet collocation method of time dependent Maxwell's equations: Characterization of electrically-large optical waveguide discontinuities," *J. Comp. Phys.*, vol. 186/2, pp. 666–689, 2003.

[4] T. Hirono, Y. Shibata, W. W. Lui, S. Seki, and Y. Yoshikuni, "The second-order condition for the dielectric interface orthogonal to the Yee-latice axis in the FDTD scheme," *IEEE Microwave Guided Wave Lett.*, vol. 10, pp. 359–361, Sept. 2000.

[5] K.-P. Hwang and A. Cangellaris, "Effective permittivities for second-order accurate FDTD equations at dielectric interfaces," *IEEE Microwave Wireless Comp. Lett.*, vol. 11, no. 4, pp. 158–160, Apr. 2001.

[6] N. Kaneda, B. Houshmand, and T. Itho, "FDTD analysis of dielectric resonators with curved surfaces," *IEEE Trans. Microwave Theory Tech.*, vol. 45, pp. 1645–1649, Sept. 1997.

[7] S. Dey and R. Mittra, "A conformal finite-difference time-domain technique for modeling cylindrical dielectric resonators," *IEEE Trans. Microwave Theory Tech.*, vol. 47, pp. 1737–1739, Sept. 1999.

[8] W. Yu and R. Mittra, "A conformal finite difference time domain technique for modeling curved dielectric surfaces," *IEEE Microwave Wireless Comp. Lett.*, vol. 11, pp. 25–27, Jan. 2001.